



HAL
open science

Hierarchical clustering of spectral images with spatial constraints for the rapid processing of large and heterogeneous datasets from ancient material studies

Serge Cohen, Gilles Celeux, Agnès Grimaud, Pierre Gueriau, Sajjad Mahdavi

► **To cite this version:**

Serge Cohen, Gilles Celeux, Agnès Grimaud, Pierre Gueriau, Sajjad Mahdavi. Hierarchical clustering of spectral images with spatial constraints for the rapid processing of large and heterogeneous datasets from ancient material studies. GRC : Scientific Methods in Cultural Heritage Research, Jul 2022, Les Diablerets, Switzerland. . hal-04420576

HAL Id: hal-04420576

<https://cnrs.hal.science/hal-04420576v1>

Submitted on 26 Jan 2024

HAL is a multi-disciplinary open access archive for the deposit and dissemination of scientific research documents, whether they are published or not. The documents may come from teaching and research institutions in France or abroad, or from public or private research centers.

L'archive ouverte pluridisciplinaire **HAL**, est destinée au dépôt et à la diffusion de documents scientifiques de niveau recherche, publiés ou non, émanant des établissements d'enseignement et de recherche français ou étrangers, des laboratoires publics ou privés.

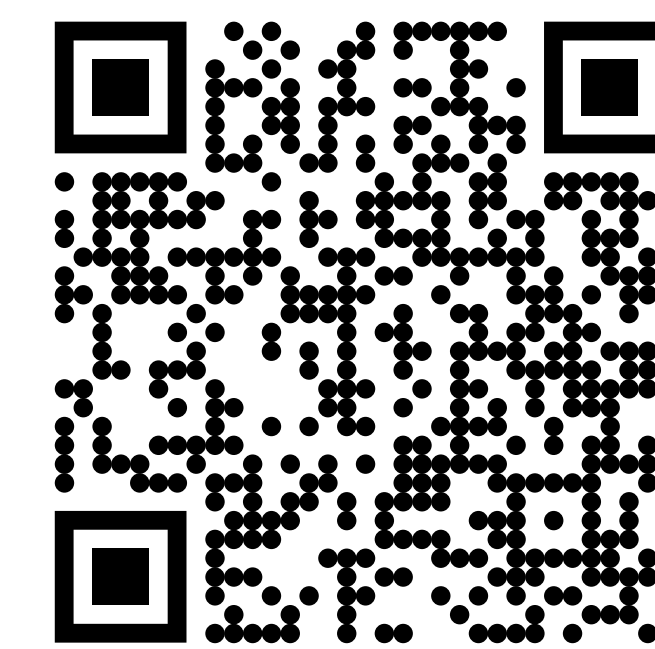
Hierarchical clustering of spectral images with spatial constraints for the rapid processing of large and heterogeneous datasets from ancient material studies

Gilles Celeux², Serge X. Cohen¹, Agnès Grimaud³, Pierre Gueriau¹, Sajjad Mahdavi¹

¹IPANEMA, UAR 3461 CNRS / Ministère de la Culture / MNHN / Université de Versailles Saint-Quentin, Gif-sur-Yvette, France

²IMO, UMR 8628 Inria, CNRS / Université Paris-Saclay, Orsay, France

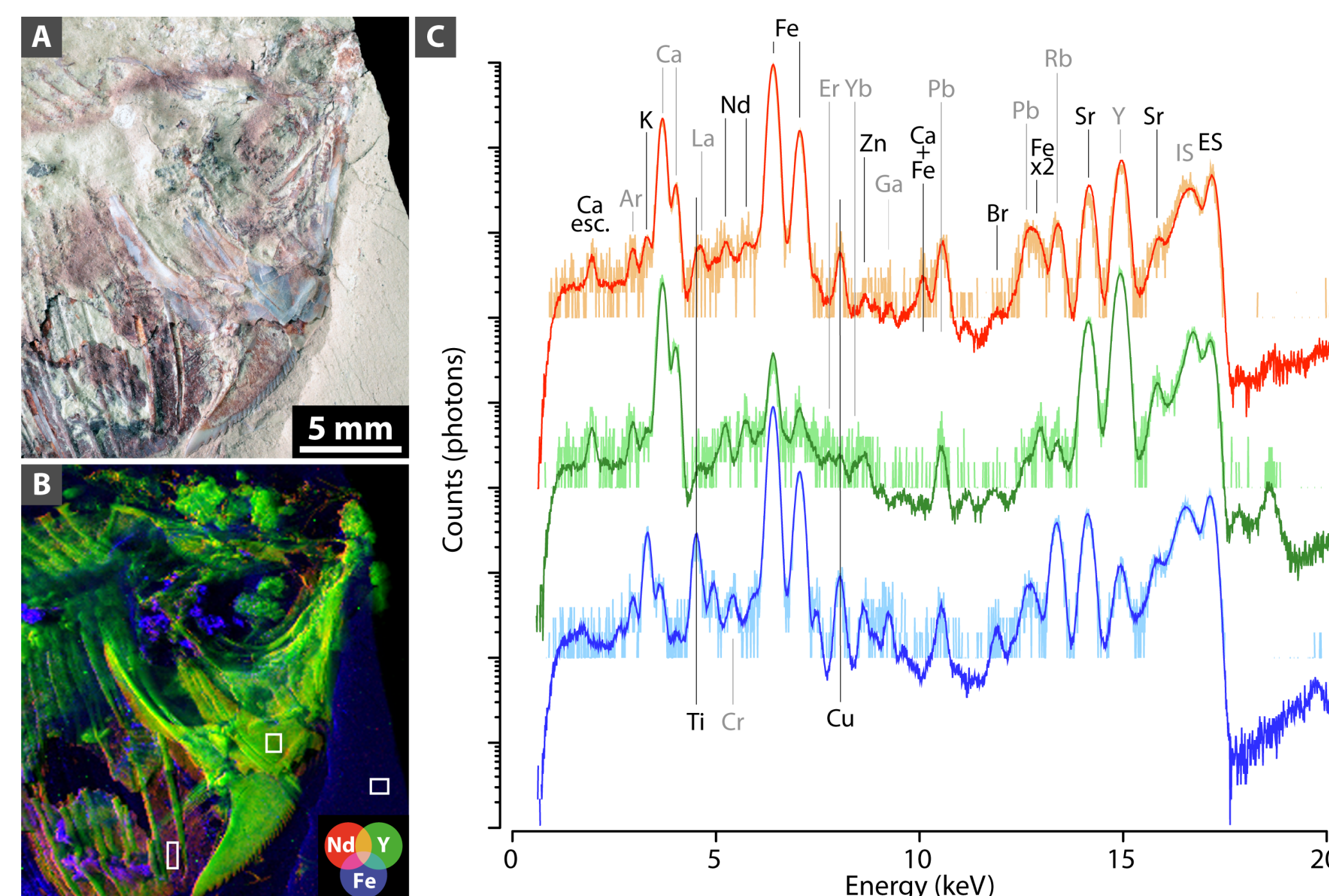
³LMQ, UMR 8100, CNRS / Université de Versailles Saint-Quentin, Versailles, France



01 Abstract

The study of very complex and heterogeneous materials, such as those encountered in the science of ancient materials, benefits from the wealth of information provided by the acquisition and exploitation of full spectrum images, *i.e.* spectral images. In order to obtain a high dynamic range in both the spatial and compositional dimensions, great efforts have made it possible to considerably accelerate data collection and increase the average size of a single data set, each image reaching up to several tens of GB. Rapid processing is now required to allow feedback during data collection, within the short time available for instruments and samples. Here we propose an approach combining hierarchical clustering and spatial constraint. Spatial constraints allow both a significant reduction in the computational cost of segmentation and a certain level of robustness with respect to the signal-to-noise ratio: the *prior* knowledge injected by the spatial constraint partially compensates for the increase in noise level; hierarchical clustering provides a statistically sound and known framework that allows accurate reporting of the instrument noise model. We illustrate the proposed algorithm on a X-ray fluorescence spectral image collected on an *ca.* 100 Myr fossil fish, as well as on simulated data to assess the sensitivity of the results to the noise level. It can be foreseen how such an approach could simultaneously lead to an increase in the spatial definition of the collected spectral image and to a reduction in the potentially harmful radiation dose density to which the samples are subjected.

02 Typical dataset



Synchrotron XRF mapping of major-to-trace elements of the anterior part (skull on the right) of the yet undescribed fish MHNM-KK-OT 03a from the Jbel Oum Tkout Lagerstätte (Upper Cretaceous, 100 Myr, Morocco). (a): optical photograph. (b): false color overlay of the distributions of two rare earth elements, neodymium (red) and yttrium (green), and of iron (blue), reconstructed from a full spectral decomposition of the data. Acquisition parameters: 100 x 100 μm^2 scan step, 50,851 pixels. (c): Mean (dark colored; 90 pixels) and central individual (light colored) spectra from the boxes in b, corresponding to fossilized muscles (red), bone (green) and the sedimentary matrix (blue), respectively. Spectra are shown using a logarithmic scale, vertically shifted for clarity. Main peaks are labelled. Abbreviations: esc., escape peak; ES, elastic scattering; IS, inelastic scattering; x2, sum (double) peak. Note that the Ar-peak does not arise from the sample but is due to excitation of Ar in the air (*ca.* 0.93 %) between the sample and the detector.

03 Statistically oriented processing of XRF spectra scans

We consider each XRF spectra as a random sample of the population of photon that are emitted under X-ray excitation of the elementary volume. We, hence, use tools adapted to the comparison of population samples. we propose is based on the χ^2 as a tool to assess homogeneity between two samples.

$$d_{\chi^2}^2(S_i, S_j) = \sum_{p=1}^P \frac{(t_p^i - t_p^j)^2}{f_{\cdot p}}$$

This is naturally extended to comparing two sets of pixels :

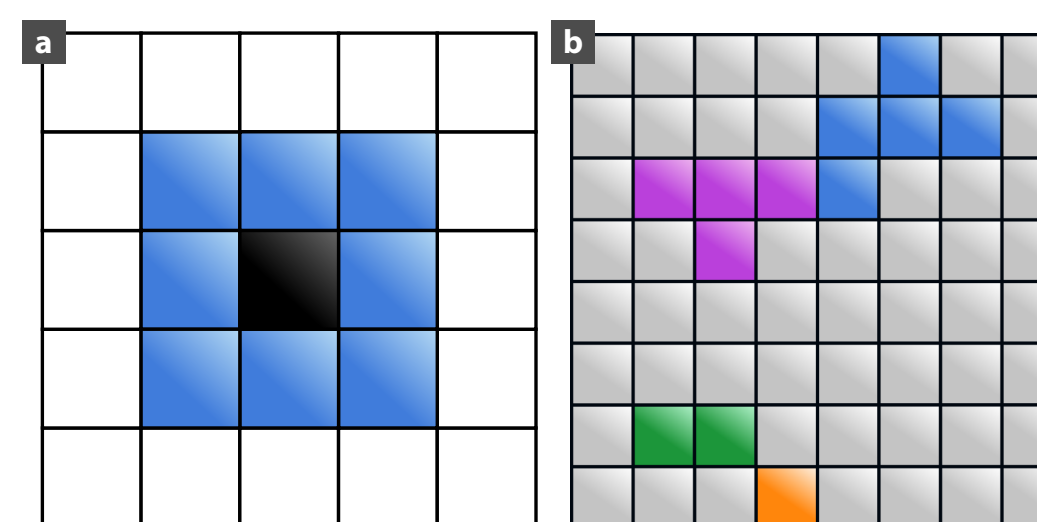
$$\delta_{\chi^2}(C, C') = \frac{\mu_C \mu_{C'}}{\mu_C + \mu_{C'}} d_{\chi^2}^2(S_{g_C}, S_{g_{C'}})$$

An aggregation of two classes leads to :

$$S_{g_{C \cup C'}} = \frac{\mu_C S_{g_C} + \mu_{C'} S_{g_{C'}}}{\mu_C + \mu_{C'}} \quad \mu_{C \cup C'} = \mu_C + \mu_{C'}$$

04 Imposing spatial constraints

Schematic representation of the second-order neighborhoods approach. (a): neighbors for a pixel that is not located on an edge or at a corner. (b): example of clusters spatially neighboring: on the top, the blue and purple clusters are spatially neighboring, while on the bottom left the green and orange clusters are spatially neighboring. All are spatially neighboring to the grey cluster. On another hand, for example, the purple and orange clusters are not spatially neighboring.

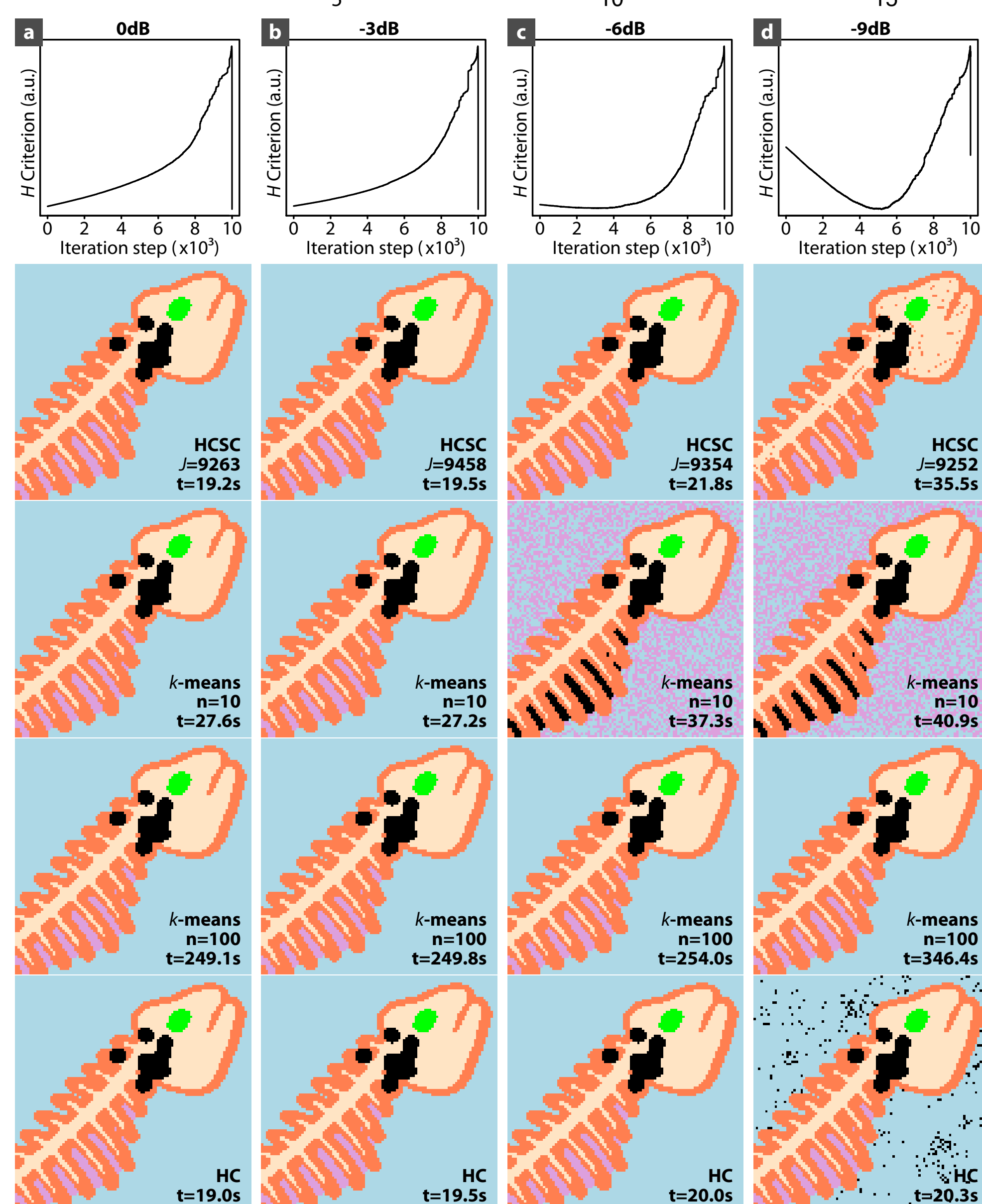
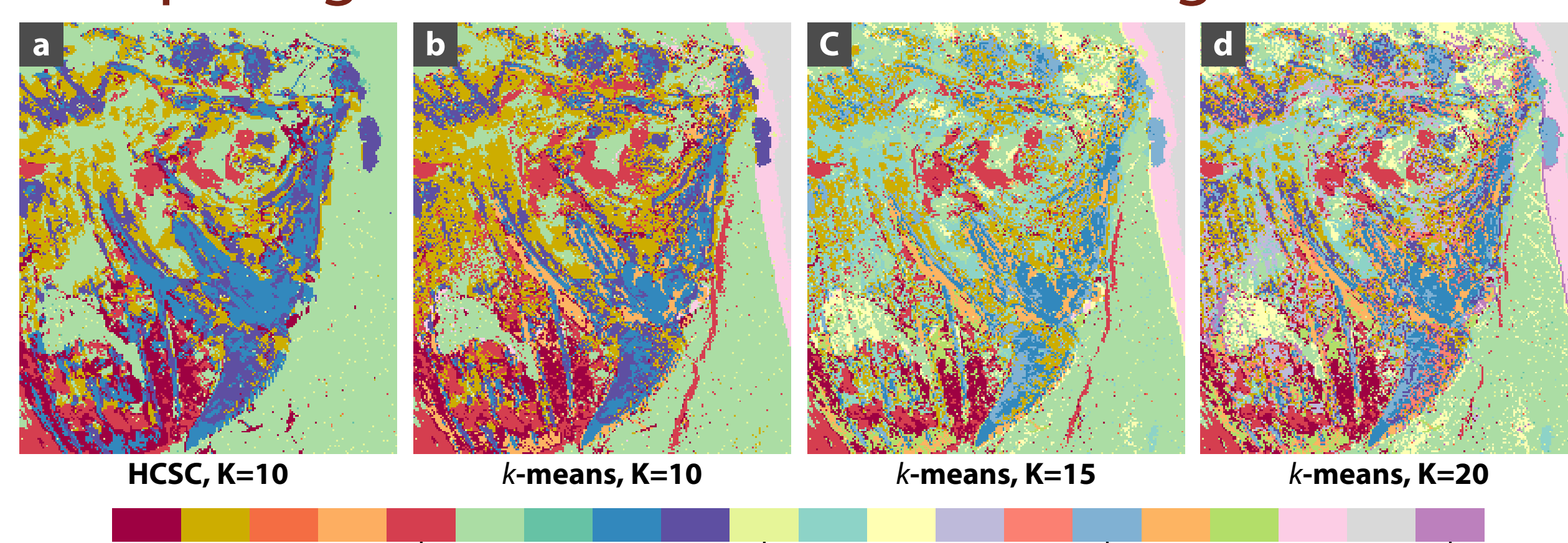


05 Algorithm

Initialization : computes the χ^2 distances between two spectra for neighboring pixels
 Define $L := 1$
 while $L < N$ do
 Aggregates the two neighboring clusters with the smallest Ward criterion value (or χ^2 distances at the first step)
 Updates the neighborhoods of clusters.
 Updates the dissimilarity matrix (for spatially neighboring clusters).
 $L := L + 1$
 end while



07 Comparing to more classical clustering methods



Assessing effectiveness and efficiency of the proposed algorithm on a synthetic dataset for which ground truth is known

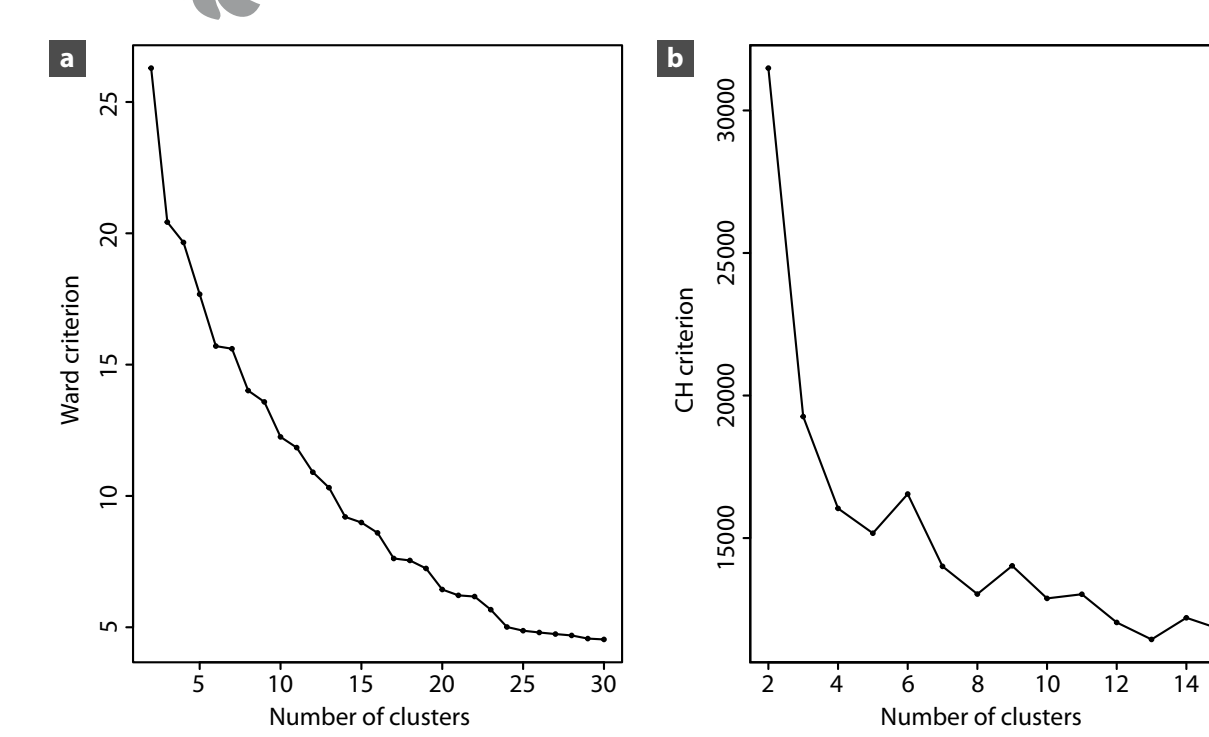
Building the synthetic dataset:

We drew a fossil composed of six classes, namely sediment, bone, bone coating, muscles, eye and iron-rich grains. Each of those classes is assigned a reference spectrum taken from the mean spectra of the clusters identified above using HCSC (these mean spectra are obtained from a large number of pixels and hence exhibit the strong regularity of noiseless spectra). Each pixel is then assigned the reference spectrum of its class multiplied by an amplitude factor being the exponential of a zero-mean Gaussian random field of appropriate variance and spatial regularity. This synthetic model provides ground truth both in terms of class and spectrum for each pixel.

We, then, can generate a simulated observed spectra with the same SNR as the raw observation, by simply replacing the value of the above model (*zero noise spectra*) by a single realization of a Poisson random process with its parameter being the model's value.

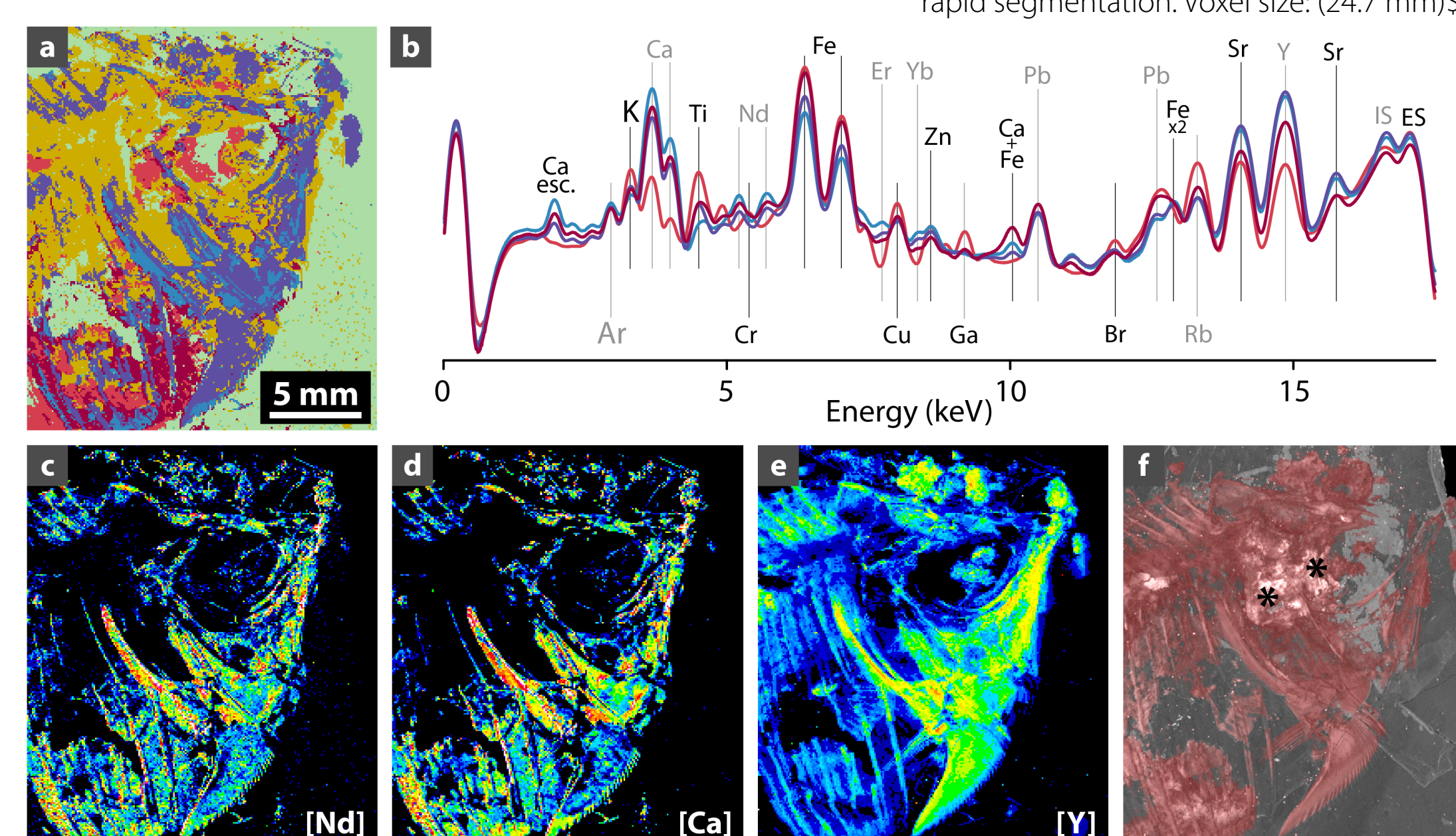
Effectiveness and efficiency of our hierarchical clustering with spatial constraints as compared to that of *k-means* (with both 10 and 100 initializations) and standard hierarchical clustering (HC) on the purely synthetic data set, when removing 0dB (a), 3dB (b), 6dB (c) and 9dB (d) to the SNR

06 Produced segmentation

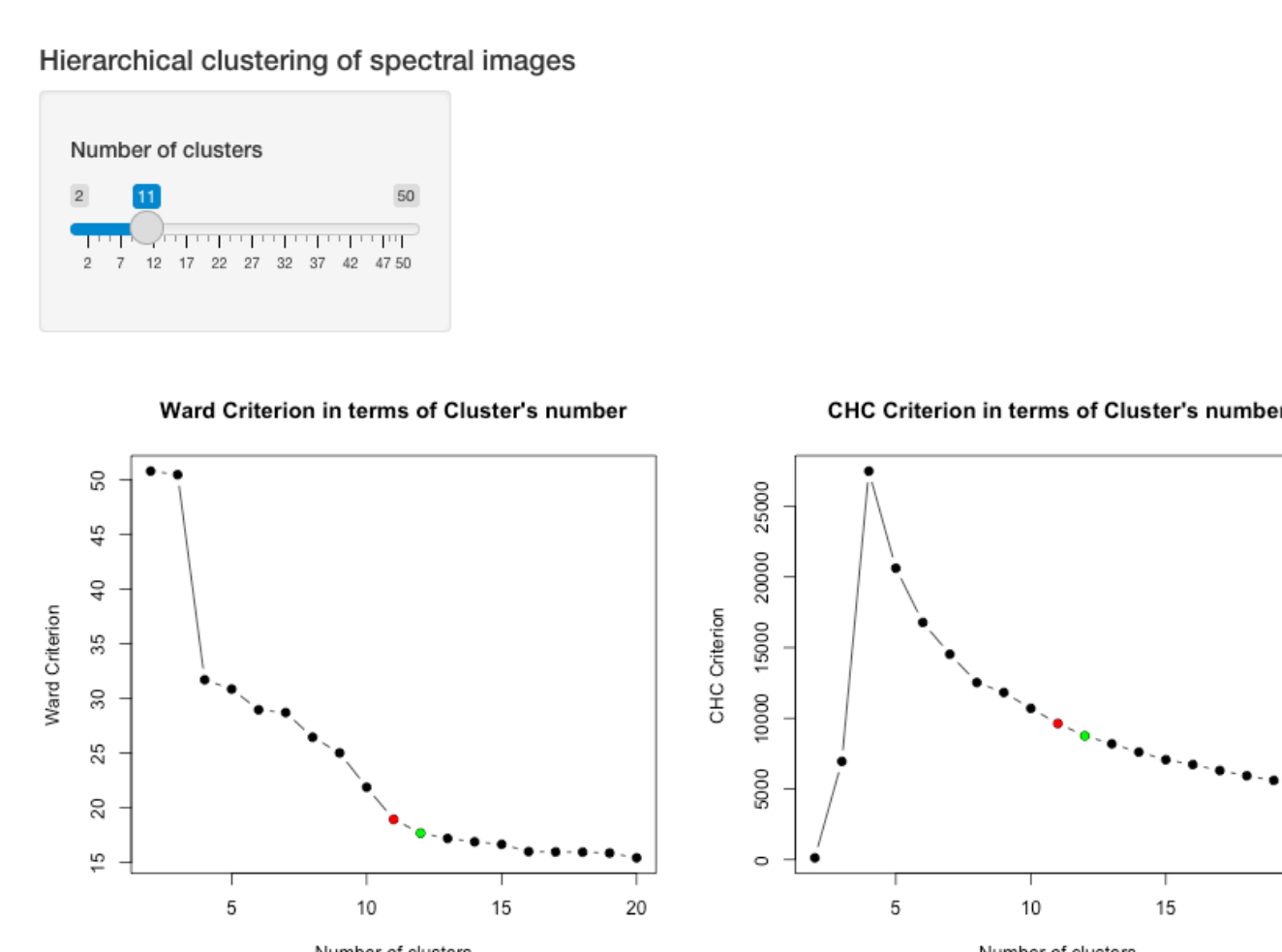


Defining the number of clusters used for hierarchical segmentation (a, b): Ward (a) and Calinski and Harabasz (b) criteria against the number of clusters (starting with 2 clusters). (c-e): False color distributions obtained for 5 (c) and 10 (d) clusters, and difference (e)

(a): Segmentation results when 10 clusters are selected with the proposed algorithm, disabling spatial constraint at step $J=44175$. (b): mean spectra from 4 of the 10 clusters visible in (a). (c-e): concentration maps of neodymium (c), calcium (d) and yttrium (e). The color scale goes from dark blue (for low concentration) to red (high concentration) going through green and yellow. (f): micro-computed tomography 3D rendering of the fossil within the sedimentary matrix after rapid segmentation. Voxel size: $(24.7 \text{ nm})^3$



08 A graphical exploratory interface



*E-mail: serge.cohen@ipanema-remote.fr